

# Promotion of Low-Temperature Reduction Behavior of the $\text{CeO}_2\text{--ZrO}_2\text{--Bi}_2\text{O}_3$ Solid Solution by Addition of Silver

Nobuhito Imanaka,\* Toshiyuki Masui,  
Keisuke Minami, and Kazuhiko Koyabu

Department of Applied Chemistry, Faculty of Engineering,  
Osaka University, 2-1 Yamadaoka,  
Suita, Osaka 565-0871, Japan

Received August 27, 2005

Revised Manuscript Received November 10, 2005

Within the field of solid-state chemistry, oxygen storage and release properties of cerium oxides ( $\text{CeO}_2$ ) have played important roles, especially in terms of automotive exhaust catalysts.<sup>1</sup>  $\text{CeO}_2$  and its related materials can lower the ignition temperatures of particulate matters (mainly soot) that are released from diesel vehicles.<sup>2</sup> Soot emission is a significant component of air pollution and is harmful for both human beings and the environment. In recent years, therefore, much attention has been given on the synthesis and characterization of solid solutions based on  $\text{CeO}_2$ . In particular, studies have focused on  $\text{CeO}_2\text{--ZrO}_2$ , which possess significantly enhanced thermal stability, redox property, and catalytic activities (comparable to those of pure  $\text{CeO}_2$ ).<sup>3</sup>

Reduction behavior at low temperatures and high degree of reducibility of  $\text{CeO}_2\text{--ZrO}_2$  solid solutions are attractive properties in regards to automotive exhaust catalysts. Numerous investigations<sup>1,3</sup> have been carried out to determine the optimal composition, structure, and morphology of the  $\text{Ce}_x\text{Zr}_{1-x}\text{O}_2$  solid solutions.<sup>1,3</sup> Other studies have aimed at investigating the effect of trivalent dopants such as yttria,<sup>2,4,5</sup> lanthana,<sup>4</sup> and praseodymia<sup>6</sup> on the redox behavior of the  $\text{Ce}_x\text{Zr}_{1-x}\text{O}_2$  materials. However, tests show the difficulty for such conventional materials to retain their reduction behavior at low temperatures after oxidation at high temperatures (above 900 °C). Surface etching, a known solution to this problem,<sup>7</sup> did not substantially improve the reduction behavior of these materials.

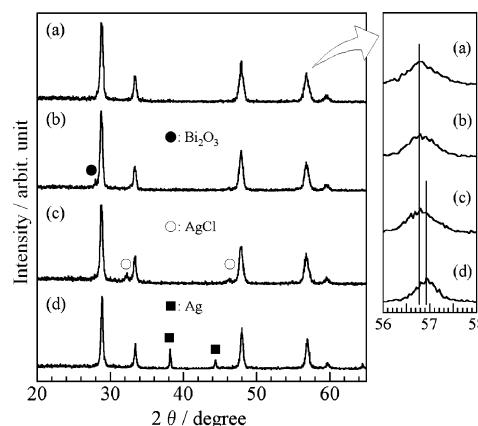


**Figure 1.** X-ray powder diffraction patterns of the  $\text{Ce}_{0.68}\text{Zr}_{0.17}\text{Bi}_{0.15}\text{O}_{1.925}$  (CZB) and the  $0.84\text{Ce}_{0.68}\text{Zr}_{0.18}\text{Bi}_{0.14}\text{O}_{1.93}\cdot 0.16\text{AgCl}$  (CZB-Ag) catalysts: (a) as-prepared CZB, (b)  $\text{Ce}_{0.68}\text{Zr}_{0.17}\text{Bi}_{0.15}\text{O}_{1.925}$  after 10 cycles of reduction and subsequent reoxidation treatment (CZB\_aged), (c) as-prepared CZB-Ag, and (d)  $0.84\text{Ce}_{0.68}\text{Zr}_{0.18}\text{Bi}_{0.14}\text{O}_{1.93}\cdot 0.16\text{AgCl}$  after 10 cycles of reduction and subsequent reoxidation treatment (CZB-Ag\_aged).

Previously, we have proposed that the introduction of small amounts of  $\text{Bi}_2\text{O}_3$  within the  $\text{CeO}_2\text{--ZrO}_2$  lattice may effectively allow the solid solution to maintain its reduction behavior at low temperatures (below 300 °C).<sup>8</sup> Unfortunately, treatment of  $\text{CeO}_2\text{--ZrO}_2\text{--Bi}_2\text{O}_3$  to repeated cycles of reduction and reoxidation (redox aging) at 900 °C resulted in an increase in the reduction temperature. Subsequently, we discovered that the addition of silver, which is well-known as an oxygen-permeable material,<sup>9</sup> into the  $\text{CeO}_2\text{--ZrO}_2\text{--Bi}_2\text{O}_3$  solid solution was effective in maintaining the mixture's low-temperature reduction behavior. Herein, we present the effects of silver on the retention of the low-temperature reduction behavior of  $\text{CeO}_2\text{--ZrO}_2\text{--Bi}_2\text{O}_3$ .

X-ray fluorescence analyses were carried out on  $\text{Ce}_{0.68}\text{Zr}_{0.17}\text{Bi}_{0.15}\text{O}_{1.925}$  (denoted CZB hereafter), which was synthesized by a coprecipitation method, and on  $0.84\text{Ce}_{0.68}\text{Zr}_{0.18}\text{Bi}_{0.14}\text{O}_{1.93}\cdot 0.16\text{AgCl}$  (denoted CZB-Ag hereafter), which was prepared by heating a ball-milled mixture of AgCl and  $\text{Ce}_{0.68}\text{Zr}_{0.17}\text{Bi}_{0.15}\text{O}_{1.925}$  obtained by coprecipitation. The X-ray powder diffraction pattern (XRD) of CZB (Figure 1a) displayed only diffraction peaks that are attributable to a cubic fluorite-type structure, whereas the diffraction pattern for the AgCl-added sample (CZB-Ag) (Figure 1c) exhibited a small amount of the AgCl phase as a secondary phase. In addition, CZB-Ag was identified as a simple mixture because the diffraction angles for the fluorite peaks of CZB and CZB-Ag coincided, that is, peak shifts were not observed between the profiles.

The temperature-programmed reduction (TPR) trace of CZB displayed a reduction peak at 264 °C (Figure 2a). The

\* Corresponding author. Telephone: +81 (0)6 6879 7352. Fax: +81 (0)6 6879 7354. E-mail: imanaka@chem.eng.osaka-u.ac.jp.

- (1) Taylor, K. C. *Automobile catalytic converters*. In *Catalysis—Science and Technology*; Anderson, J. R., Boudart, M., Eds.; Springer-Verlag: Berlin, 1984; Vol. 5. (b) Kašpar, J.; Fornasiero, P.; Graziani, M. *Catal. Today* **1999**, *50*, 285. (c) Trovarelli, A. *Catalysis by Ceria and Related Materials*; Imperial College Press: London, 2002.
- (2) Lamonier, J. F.; Kulyova, S. P.; Zhikinskaya, E. A.; Kostyuk, B. G.; Lumin, V. V.; Aboukaxos, A. *Kinet. Catal.* **2004**, *45*, 429.
- (3) (a) Ozawa, M.; Kimura, M.; Isogai, A. *J. Alloys Compd.* **1993**, *193*, 73. (b) Kašpar, J.; Fornasiero, P.; Hickey, N. *Catal. Today* **2003**, *77*, 419. (c) Kašpar, J.; Fornasiero, P. *J. Solid State Chem.* **2003**, *171*, 19. (d) Di Monte, R.; Kašpar, J. *Catal. Today* **2005**, *100*, 27. (e) Di Monte, R.; Kašpar, J. *J. Mater. Chem.* **2005**, *15*, 633.
- (4) (a) Vidmar, P.; Fornasiero, P.; Kašpar, J.; Gubitosa, G.; Graziani, M. *J. Catal.* **1997**, *171*, 160. (b) Ikryannikova, L. N.; Aksenov, A. A.; Markaryan, G. L.; Muravieva, G. P.; Kostyuk, B. G.; Kharlanov, A. N.; Lunina, E. V. *Appl. Catal. A* **2001**, *210*, 225.
- (5) (a) Markaryan, G. L.; Ikryannikova, L. N.; Muravieva, G. P.; Turakulova, A. O.; Kostyuk, B. G.; Lunina, E. V.; Lunin, V. V.; Zhilinskaya, E.; Aboukais, A. *Colloids Surf. A* **1999**, *151*, 435. (b) Settu, T.; Gobinathan, R. *J. Eur. Ceram. Soc.* **1996**, *16*, 1309.
- (6) Narula, C. K.; Haack, L. P.; Chun, W.; Jen, H.-W.; Graham, G. W. *J. Phys. Chem. B* **1999**, *103*, 3634.

- (7) (a) Masui, T.; Nakano, K.; Ozaki, T.; Adachi, G.; Kang, Z.; Eyring, L. *Chem. Mater.* **2001**, *13*, 1834. (b) Ozaki, T.; Masui, T.; Machida, K.; Adachi, G.; Sakata, T.; Mori, H. *Chem. Mater.* **2000**, *12*, 643. (c) Kašpar, J.; Di Monte, R.; Fornasiero, P.; Graziani, M.; Bradshaw, H.; Norman, C. *Top. Catal.* **2001**, *16*–17, 83.
- (8) Minami, K.; Masui, T.; Imanaka, N.; Dai, L.; Pacaud, B. *J. Alloys Compd.* (available online 14 June 2005).
- (9) Beavis, L. C. *Rev. Sci. Instrum.* **1972**, *43*, 122.

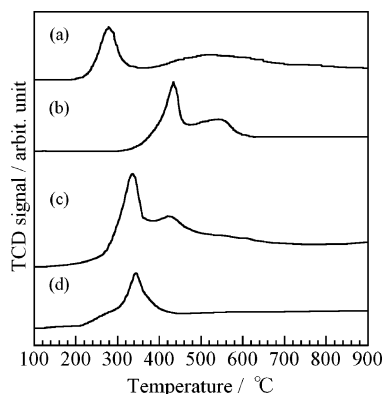


**Figure 2.** Temperature-programmed reduction profiles of the catalysts: (a) CZB, (b) CZB\_aged, (c) CZBAG, and (d) CZBAG\_aged.

oxide resulting from the TPR treatment in Figure 2a was reoxidized by a pulse technique, in which the oxygen storage capacity (OSC) value was  $696 \mu\text{mol of O}_2 \text{ g}^{-1}$ . The TPR diagram after 10 cycles of redox aging is shown in Figure 2b. The significant upward shift (in temperature) of the main reduction peak, relative to the profile of the as-prepared sample, implies that the reducibility of the sample has deteriorated considerably. Despite the increase of the OSC value to  $906 \mu\text{mol of O}_2 \text{ g}^{-1}$ , the reduction temperature rose to  $434^\circ\text{C}$ . After 10 cycles of redox aging, segregation of  $\text{Bi}_2\text{O}_3$  was detected in the XRD pattern of  $\text{Ce}_{0.68}\text{Zr}_{0.17}\text{Bi}_{0.15}\text{O}_{1.925}$  (Figure 1b). This catalyst is termed “CZB\_aged” hereafter. This deposition induced the decreasing of Bi content in the solid solution, which leads to the rise of the reduction temperature. On the contrary, the  $\text{Bi}_2\text{O}_3$  segregation correlates with the increase in the oxygen storage capacity because pure  $\text{Bi}_2\text{O}_3$  is easily reduced around  $500^\circ\text{C}$ .

In contrast, the TPR trace of the CZBAG (Figure 2c) indicated a reduction behavior at around  $340^\circ\text{C}$ . Although the CZBAG was a mixture of CZB and AgCl (Figure 1c), these compounds were vigorously mixed by mechanical ball-milling and strongly contacted each other. The AgCl particles adhered on the surface of the CZB will inhibit the low-temperature reduction. Consequently, the reduction peak of the CZB material ( $264^\circ\text{C}$ ) increased to  $340^\circ\text{C}$  with the addition of AgCl. However, this reduction behavior was unaffected by 10 cycles of redox aging (as depicted in Figure 2d). The redox-aged CZBAG sample is termed “CZBAG\_aged” hereafter.

To identify the origin of the different reduction behaviors described above, Raman spectra of the compounds were measured and are shown in Figure 3. The Raman spectrum of CZB exhibited a strong band at  $467 \text{ cm}^{-1}$ , which was assigned to the  $F_{2g}$  mode of a cubic fluorite structure, and two minor peaks at 313 and  $573 \text{ cm}^{-1}$ . Such spectral features are indicative of a  $t'$  phase, which is a type of a tetragonal structure containing oxygen displacement within the fluorite lattice.<sup>10</sup> Although the Raman trace was not affected by the redox aging, a small amount of  $\text{Bi}_2\text{O}_3$  deposition was detected in the XRD pattern, as shown in Figure 1b. On the other hand, the Raman spectrum of the CZBAG\_aged sample exhibited a remarkable behavior—after 10 cycles of redox

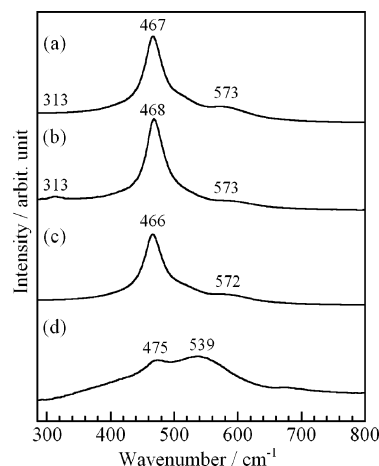


**Figure 3.** Raman spectra of the catalysts: (a) CZB, (b) CZB\_aged, (c) CZBAG, and (d) CZBAG\_aged.

aging, a new strong broad band ( $539 \text{ cm}^{-1}$ ) corresponding to the Ag—O vibration appeared.<sup>11</sup>

Surface analysis using X-ray photoelectron spectroscopy (XPS) has been carried out for the CZBAG\_aged catalyst. The result is illustrated in the Supporting Information. The XPS spectrum shows two Ag( $3d_{5/2}$ ) peaks at 367.7 and  $368.0 \text{ eV}$ , which elucidates that Ag is present both in +1 ( $367.7 \text{ eV}$ ) and 0 ( $368.0 \text{ eV}$ ) states in the catalyst.<sup>12</sup> Although  $\text{Ag}_2\text{O}$  exhibits the Ag( $3d_{5/2}$ ) peak at  $367.7 \text{ eV}$ ,  $\text{Ag}_2\text{O}$  decomposes to silver metal at  $400^\circ\text{C}$ .<sup>13,14</sup> Furthermore, the XRD pattern of the CZBAG\_aged sample indicated formation of metallic silver (Figure 1d), and no  $\text{Ag}_2\text{O}$  peaks were observed. Also, it has been confirmed that XRD peaks of the CZB phase shifted to higher angles after the redox aging as evidenced in the inset of Figure 1, by the formation of oxide anion vacancies accompanying with the silver dissolution. Therefore, it can be concluded that Ag somewhat dissolves into the CZB lattice after 10 cycles of redox aging.

The as-prepared CZBAG catalyst was a simple mixture of CZB and AgCl, and the addition of AgCl induced the increasing of the initial reduction temperature from  $264$  to  $340^\circ\text{C}$ . If there are no synergetic effects between silver dissolved in the solid solution and deposited on the surface after the redox aging, the aged catalyst should have shown the same behavior as that observed in the catalyst without Ag, that is, the reduction temperature will furthermore increase after the aging process. Accordingly, the retention of the low-temperature reduction behavior of the CZBAG\_aged could be attributed to the synergetic effects of partial dissolution of silver into the CZB lattice and the surface deposition of metallic silver on the solid solution.

The OSC values of the CZBAG and the CZBAG\_aged samples were  $951$  and  $732 \mu\text{mol of O}_2 \text{ g}^{-1}$ , respectively. The partial dissolution of silver ions into the CZB lattice produces oxide anion vacancies to maintain charge competition. The formation of the vacancy will enhance the oxide anion mobility, but the total amount of oxygen in the lattice

(10) Yashima, M.; Arashi, H.; Kakihana, M.; Yoshimura, M. *J. Am. Ceram. Soc.* **1994**, *77*, 1067.

(11) Millar, G. J.; Nelson, M. L.; Uwins, P. J. R. *Catal. Lett.* **1997**, *43*, 97.

(12) Bera, P.; Patil, K. C.; Hegde, M. S. *Phys Chem. Chem. Phys.* **2000**, *2*, 3715.

(13) Weaver, J. F.; Hoflund, G. B. *J. Phys. Chem.* **1994**, *98*, 8519.

(14) Weaver, J. F.; Hoflund, G. B. *Chem. Mater.* **1994**, *6*, 1693.

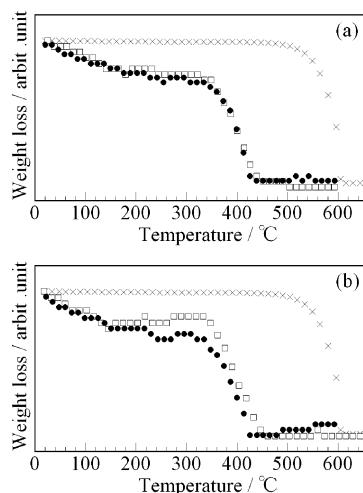


**Figure 4.** Thermogravimetric analysis curves of carbon black combustion for CZB ( $\square$ ) and CZBAg ( $\bullet$ ) catalysts: (a) as-prepared samples and (b) aged samples after 10 cycles of the reduction and subsequent reoxidation treatment. The symbol  $\times$  corresponds to the result for the combustion of carbon black itself in the absence of the catalysts.

decreases, which leads to the decrease in the total oxygen storage capacity.

The oxidation activity of the catalysts was examined from the standpoint of their ability to lower the combustion temperature of soot in air, which is about 600 °C in the absence of the catalysts.<sup>8</sup> Thermogravimetric (TG) curves for soot combustion in the presence and absence of the oxide catalysts are shown in Figure 4. The weight loss on the TG curves indicates the temperature range for the combustion of soot particulates.

Our results indicate good correlation between the weight loss and the reactivity of the bulk oxygen of the catalyst. Because the reduction temperatures of the initial CZB and CZBAg catalysts are comparable, combustion of soot occurs

at the same temperature, as depicted in Figure 4a. After 10 cycles of redox aging, however, differences in the combustion temperatures were observed (Figure 4b)—the soot combustion temperature for the CZB catalyst increased slightly because of the higher temperature at which the active oxygen was released from this sample by aging. These profiles can be reproduced within the experimental deviation of  $\pm 2$  °C. As shown in Figure 4, the lattice oxygen of the catalyst can participate in soot oxidation, and the reactivity of oxygen in the bulk of the catalyst highly improves the combustion activities.

In summary, retention of low-temperature reduction behavior of  $\text{CeO}_2\text{--ZrO}_2\text{--Bi}_2\text{O}_3$  was realized by the addition of silver to the solid solution. On the basis of our results, it can be suggested that the synergistic effects of the partial solution and surface deposition of silver are responsible for maintaining the activity, in which the oxygen permeability of silver enhances low-temperature reduction, even after 10 cycles of redox aging.

**Acknowledgment.** The authors sincerely thank Prof. Kuniaki Murase and Prof. Yasuhiro Awakura (Kyoto University) for their assistance with the Raman spectra measurements. The present work was supported by Grant-in-Aid for Scientific Research 17350100 from the Japan Society for the Promotion of Science (JSPS) and by the Industrial Technology Research Grant Program in 02 (Project 02A27004c) from the New Energy and Industrial Technology Development Organization (NEDO) based on funds provided by the Ministry of Economy, Trade and Industry, Japan (METI).

**Supporting Information Available:** Experimental details and instrumentations. This material is available free of charge via the Internet at <http://pubs.acs.org>.

CM0519380